



## OPEN ACCESS

## EDITED BY

Felix Ngosa Toka,  
Ross University School of Veterinary  
Medicine, Saint Kitts and Nevis

## REVIEWED BY

Thiago J. Borges,  
Massachusetts General Hospital and  
Harvard Medical School, United States  
Jeremy Alastair O'Sullivan,  
Northwestern University, United States

## \*CORRESPONDENCE

Guoxing Wang  
✉ [guoxing.wang@sanofi.com](mailto:guoxing.wang@sanofi.com)

RECEIVED 09 December 2025

REVISED 18 February 2026

ACCEPTED 19 February 2026

PUBLISHED 17 March 2026

## CITATION

Keeney JN, Schwarte J, Yang B,  
Wesseling H, Zhang B, McKnight AJ,  
Hegde S and Wang G (2026) Siglec-7  
inhibits TLR3-induced pro-inflammatory  
cytokine production from human  
monocytes and macrophages.  
*Front. Immunol.* 17:1764343.  
doi: 10.3389/fimmu.2026.1764343

## COPYRIGHT

© 2026 Keeney, Schwarte, Yang,  
Wesseling, Zhang, McKnight, Hegde and  
Wang. This is an open-access article  
distributed under the terms of the  
[Creative Commons Attribution License  
\(CC BY\)](https://creativecommons.org/licenses/by/4.0/). The use, distribution or  
reproduction in other forums is  
permitted, provided the original  
author(s) and the copyright owner(s) are  
credited and that the original publication  
in this journal is cited, in accordance  
with accepted academic practice. No  
use, distribution or reproduction is  
permitted which does not comply with  
these terms.

# Siglec-7 inhibits TLR3-induced pro-inflammatory cytokine production from human monocytes and macrophages

Justin N. Keeney<sup>1,2</sup>, Janina Schwarte<sup>3</sup>, Bo Yang<sup>4</sup>,  
Hendrik Wesseling<sup>4</sup>, Bailin Zhang<sup>4</sup>, Andrew J. McKnight<sup>1</sup>,  
Subramanya Hegde<sup>1</sup> and Guoxing Wang<sup>1\*</sup>

<sup>1</sup>Immunology & Inflammation Research, Sanofi R&D, Cambridge, MA, United States, <sup>2</sup>Sanofi Global Postdoctoral Fellowship Program, Cambridge, MA, United States, <sup>3</sup>Target, Disease & Systems Biology, Sanofi R&D, Cambridge, MA, United States, <sup>4</sup>Translational Medicine Unit, Sanofi R&D, Cambridge, MA, United States

Immune checkpoint receptors, including Sialic-acid-binding immunoglobulin-like lectins (Siglecs), are critical regulators of immune homeostasis. Siglecs can serve as negative regulators of Toll-like receptor (TLR) signaling, promoting the resolution of inflammatory signaling through feedback inhibition mechanisms. Previous studies demonstrated that Siglec-E, the murine homolog of the human inhibitory receptor Siglec-7, negatively regulates TLR4 signaling by controlling receptor endocytosis. This regulatory mechanism suggests that Siglec-7 may also limit TLR signaling. Here we reveal a novel mechanism whereby Siglec-7 represses endosomal TLR3 activation, compared to other TLRs, in human myeloid cells. Crosslinking Siglec-7 with antibody clone QA79 significantly reduced TNF $\alpha$  secretion in U937 cells, primary monocytes, and macrophages following Poly(I:C) stimulation. Mechanistically, QA79 triggers rapid Fc $\gamma$ R-independent internalization and endolysosomal trafficking of surface Siglec-7, which enables the direct co-localization of Siglec-7 with TLR3 within the endolysosome. This co-localization between Siglec-7 and TLR3 suppresses NF- $\kappa$ B phosphorylation, a key pro-inflammatory signaling node downstream of TLR3. These findings establish a previously unrecognized negative regulatory role of Siglec-7 for TLR3-mediated inflammation in myeloid cells, where a disrupted interaction could contribute to autoimmune disease pathogenesis. Targeting this pathway represents a promising therapeutic approach for TLR3-driven autoimmune diseases.

## KEYWORDS

agonism and antagonism, antibody, endolysosome, glycosylation, myeloid cells, pro-inflammatory, Siglec-7, TLR3

## Introduction

Toll like receptors (TLRs) are critical first-line host defense sensors (1). Disruption of regulatory processes that control TLR activation underpins autoimmune diseases (1). Among these receptors, TLR3 localizes to the endosome and binds to double-strand RNA to induce production of type-1 interferons and pro-inflammatory cytokines (2).

Dysregulated TLR3 underlies autoimmune diseases such as Rheumatoid Arthritis, Systemic Lupus Erythematosus, and Type-1 Diabetes (2). Previous reports show Siglec family proteins can negatively regulate TLR signaling with multiple mechanisms described (3–9). Sialic-acid-binding immunoglobulin-like lectins (Siglecs) are evolutionarily conserved type-1 transmembrane proteins found on immune cells that bind to sialic acid residues on glycosylated substrates (10, 11). Multiple Siglecs, such as Siglec-7, can bind to TLR3, however the functional significance of this observation is unknown (12).

The inhibitory immune checkpoint receptor Siglec-7 is constitutively expressed on myeloid and NK cell populations (13). Siglec-7 preferentially binds to glycosylated molecules containing an  $\alpha$ 2,8,  $\alpha$ 2,6, or  $\alpha$ 2,3 terminal-linked sialic acid (14–17). These sialic acids appear on pathogenic substrates such as bacteria (18) and viruses (19–22) as well as non-pathogenic substrates such as zymosan (23) and certain self-ligands (14). Recently, CD43 expressed on T cells was identified as a novel endogenous ligand for Siglec-7 (24, 25). This bidirectional Siglec-7/CD43 crosstalk between APCs and T cells elicits tolerogenic programming of T cells, revealing a Siglec-7-mediated mechanism that negatively regulates T cell activity (26).

Emerging evidence has implicated Siglec-7 in multiple immune-mediated inflammatory conditions including relapsing-remitting Multiple Sclerosis, Type-2 Diabetes, and solid organ transplant rejection (27–29). *In vitro*, antibody-mediated agonism of Siglec-7 decreased inflammatory cytokines from GM-CSF-induced eosinophil activation and reduced IgE-mediated cell activation of mast cells and basophils (30–32). Alternatively, antagonist antibody engagement of Siglec-7 enhanced Th1 cytokine synthesis in a mixed leukocyte reaction (26). Siglec-E, the mouse homologue of human Siglec-7, is also implicated in multiple mechanistic autoimmune models (33–36). Siglec-E binds to TLR4 and negatively regulates LPS-induced pro-inflammatory cytokines by promoting TLR4 endocytosis (6). Given the high endogenous expression of Siglec-7 on myeloid cells, it remains unclear what role Siglec-7 plays on monocytes or macrophages in respect to TLR regulation.

Here we show that crosslinking Siglec-7 with antibody clone QA79 selectively reduced TLR3-mediated TNF $\alpha$  production from monocytes and macrophages, but was ineffective in reducing TNF $\alpha$  from other TLRs. Upon antibody binding, Siglec-7 was rapidly internalized in a Fc $\gamma$ R independent manner and trafficked to the endolysosome where it co-localized with TLR3 and reduced TLR3-induced NF- $\kappa$ B phosphorylation. Our findings demonstrate a unique inhibitory function of Siglec-7 and could suggest a novel therapeutic mechanism for diseases with over-active myeloid cells that result from endosomal dysfunction.

## Materials and methods

### Reagents

Functional grade mouse IgG1 isotype antibodies specific for Siglec-7 were obtained from eBiosciences (clone QA79) or

Biolegend (clone S7.7 or Ultra-LEAF IgG1 isotype control). Functional grade goat anti-mouse F(ab')<sub>2</sub> was obtained from eBioscience.

### Cell culture

#### Cell line

U937 cells were obtained from American Type Culture Collection (ATCC).

#### PBMC Isolation

Leukopaks from healthy donors were obtained from Research Blood Components (RBC). PBMCs were isolated from Leukopaks using a Miltenyi MultiMACs system with a PBMC isolation kit (Miltenyi Biotek) and frozen in C10 Freezing Media (Stem Cell Technologies).

#### Monocytes

Monocytes were isolated from frozen PBMCs using a Monocyte Isolation Kit (Stem Cell Technologies).

#### Macrophages

Monocytes were cultured with 20 ng/mL M-CSF (R&D Systems) containing RPMI media for 3 days prior to conducting a 50% fresh M-CSF media changeout and incubating for another 3 days. Cells were detached with Accutase (Stem Cell Technologies).

All cells were grown in at 37 °C with 5% CO<sub>2</sub> in RPMI media (10% FBS + 1x Penicillin-Streptomycin).

#### Flow cytometry

Whole blood was obtained from Sanofi's Donor Research Program and red blood cells were lysed with ACK buffer (Gibco). Fc block (Invitrogen) was incubated for 10 minutes before adding the antibody cocktail and stained for 30 minutes. Excess antibody was washed, and cells were incubated in Fixation Buffer (R&D Systems) overnight at 4 °C before analyzing on a Cytex Aurora. The results were plotted and analyzed using FlowJo (BD Biosciences).

U937 cells were stained similarly to whole blood. Antibodies used for profiling can be found in [Supplementary Table 1](#).

#### Cytokine profiling

2x10<sup>5</sup> U937 cells, 2x10<sup>5</sup> monocytes, or 1.5x10<sup>5</sup> macrophages were blocked using a 5% human serum (Sigma Aldrich) solution on ice for 30 minutes. The indicated concentration of IgG control, QA79, or S7.7 antibodies were diluted in the same buffer and incubated for 30 minutes on ice. Unbound antibody was washed with cold PBS and cells were resuspended in RPMI media containing 2  $\mu$ g/mL F(ab')<sub>2</sub> and the indicated concentration of TLR ligand (Invivogen). Cells were incubated at 37 °C for 24 hours. Media was collected and frozen at -80 °C until ready for analysis. ELISA-matched antibodies for TNF $\alpha$  and IFN $\alpha$ 2 were obtained

from Biolegend. TMB substrate was used to detect the peroxidase-labeled secondary antibody and was stopped with Stop Solution (R&D Systems). Absorbance was measured on a SpectraMax M5e (Molecular Devices).

For surface glycan removal, U937 cells were treated with 125 mU Neuraminidase (Sialidase from *Clostridium perfringens*, Millipore Sigma) diluted in pH 6.0 PBS for 30 minutes at 37 °C before blocking and antibody treatment described above.

Additional cytokine profiling was conducted using multiplex assays from Meso Scale Discovery.

## Internalization assay

The assay was described previously (37) and 5 µg/mL QA79 or IgG isotype control, with or without prior incubation with Fc block (Invitrogen, Cat 14-9161-73), were preincubated as described above. Briefly, 1x10<sup>5</sup> cells were resuspended in warm media before incubating in a 37 °C water bath for the indicated timepoints. Internalization was halted by returning the cells to ice and diluting in cold PBS. Once collected, the cells were stained for 30 minutes on ice. Cells were washed and then fixed in Fixation Buffer (R&D Systems) overnight at 4 °C before analyzing on a Cytex Aurora. The results were plotted and analyzed using FlowJo (BD Biosciences). Reagents used can be found in [Supplementary Table 1](#).

## Immunoblotting

5x10<sup>5</sup> U937 cells were preincubated with 25 µg/mL IgG or QA79 and treated with 1.25 µg/mL Poly(I:C) LMW and 2 µg/mL F(ab')<sub>2</sub> as described above. Once collected, cells were lysed with RIPA buffer containing protease and phosphatase inhibitors (Invitrogen). Lysate was quantified using a BCA assay kit (ThermoFisher) and ran on precast polyacrylamide gradient gels (Bio-Rad) before transferring to nitrocellulose membranes with an iBlot2 transfer system (Invitrogen). Membranes were blocked with Starting Block buffer (Invitrogen) and incubated with primary antibodies overnight at 4 °C. Membranes were washed and incubated with HRP-conjugated secondary antibodies (Jackson ImmunoResearch) before developing with SuperSignal West Pico PLUS Chemiluminescent Substrate (Invitrogen) and imaged on a Bio-Rad ChemiDoc MP Imaging System. Densitometry measurements were analyzed in Image Lab 6.1.

Phosphorylated antibodies were striped using Restore PLUS Western Blot Stripping Buffer (Invitrogen) before proceeding as described above. Antibodies can be found in [Supplementary Table 1](#).

## scRNAseq

Siglec-7 mRNA levels in human PBMCs were taken from the BLUEPRINT dataset (<https://projects.ensembl.org/blueprint/>) accessed through Omicsoft Array Studio V12.8.0.15 (Qiagen), as described previously (38).

## Proteomics

Macrophages were differentiated as described above. One-day prior to harvest, 24-well plates were coated with 15 µg/mL QA79 or IgG isotype control. Plates were washed and blocked with RPMI

media for 1 hour at 37 °C. 2x10<sup>5</sup> cells per well were plated and incubated for 3 hours. Cells were subsequently washed with PBS and frozen at -80 °C.

Proteomic sample preparation was performed using the single-pot, solid-phase-enhanced sample preparation (SP3) workflow as previously described (39). Briefly, cells were lysed in lysis buffer containing 2% SDS, 300 mM triethylammonium bicarbonate (TEAB), 300 mM NaCl, 8 M Urea, and protease/phosphatase inhibitors. Lysates were sonicated, clarified by centrifugation (21000 g, 10 minutes, 4 °C), and equal protein amounts were reduced and alkylated with 20 mM tris(2-carboxyethyl)phosphine and 40 mM 2-chloroacetamide at 60 °C for 30 minutes. Cytiva Sera-Mag hydrophilic/hydrophobic beads (1:1) were added at a 10:1 (w/w) bead-to-protein ratio, and SP3 wash steps were carried out according to the published protocol. Proteins bound to beads were digested overnight with trypsin (1:50 w/w; Promega) in 50 mM TEAB. Peptides were eluted using LC-MS grade water and 200 mM TEAB, vacuum-dried, acidified, and loaded onto Evtips according to the manufacturer's instructions.

Mass spectrometry was performed on a timsTOF HT (Bruker) coupled to an Evosep One liquid chromatography system via a CaptiveSpray nano-electrospray source. Peptides were separated on a 15 cm × 75 µm ID IonOpticks Aurora C18 column (1.6 µm particles) with an integrated CaptiveSpray emitter using the 20-samples-per-day (20 SPD) Whisper method. diaPASEF acquisition was carried out using twenty-one precursor double windows of 25 Da, covering 475–1000 m/z and 1/K0 values of 0.85–1.27 V-s/cm<sup>2</sup>. Raw data were processed by library-free direct DIA+ analysis in Spectronaut v19.8 using the SwissProt human proteome database (January 2022). Search parameters included trypsin specificity with up to two missed cleavages, fixed carbamidomethylation (C), variable methionine oxidation, and a precursor-level FDR cutoff of 1% (Q-value < 0.01). Protein abundances were globally normalized using in-house R scripts. Missing values were imputed using k-nearest neighbors (kNN), and ComBat batch correction was applied to reduce clustering driven by donor batches.

Differential expression data ([Supplementary Table 2](#)) was filtered to only include proteins with 4 or more identified peptides and a -log(pValue) above 1.3. Protein enrichment analysis was conducted with STRING version 12.0 (<https://string-db.org>) and graphed in GraphPad Prism.

## Endolysosome co-localization

1x10<sup>6</sup> U937 cells were blocked prior to incubating with 40 µg/mL IgG or QA79 and treated with 1.25 µg/mL Poly(I:C) LMW as described above. Once collected, cells were incubated with Fc block and viability dye for 10 minutes before staining with anti-Siglec-7-PE for 30 minutes on ice. Intracellular markers were stained using a FoxP3 staining kit (Invitrogen). Stained cells were analyzed on a Cytex Amnis ImageStream Mk II. Quantification of internalized Siglec-7 and co-localization with TLR3 was calculated using IDEAS v6.3. IDEAS measures receptor internalization by comparing fluorescence within a whole-cell mask to an internal-cell mask that excludes the membrane region and focuses on intracellular fluorescent signal. (<https://cytekbio.com/pages/imagestream>).

Antibodies can be found in [Supplementary Table 1](#). All antibodies were directly conjugated except for anti-TLR3 which was conjugated with a Lightning-Link Conjugation Kit (Abcam).

## Statistical analysis

Statistical analyses were carried out using GraphPad Prism and details can be found in the figure legends. The data presented in this article was considered statistically significant at  $p \leq 0.05$ .

## Results

### Siglec-7 crosslinking reduced TNF $\alpha$ and IFN $\alpha$ 2 from activated TLR3 in U937 cells

Siglec proteins are known to negatively regulate TLR function, preventing excessive inflammatory signaling (3–8). However, the specific role of myeloid expressed Siglec-7 in regulating TLR-induced cytokine production remains poorly understood. To address this knowledge gap, we used the human monocytic U937 cell line, which exhibited high endogenous Siglec-7 and TLR3 expression ([Figure 1A](#); [Supplementary Figure 1A](#)). Two Siglec-7 antibody clones with distinct functions were obtained: an agonist clone QA79 (30, 31) and antagonist clone S7.7 (26, 40, 41). TLR3 was the initial focus due to the strong binding preference of Siglec-7 for TLR3 (12). QA79-mediated Siglec-7 crosslinking, unlike S7.7, significantly reduced both TNF $\alpha$  and IFN $\alpha$ 2 in U937 cells stimulated with Poly(I:C) LMW ([Figures 1B, C](#)). Poly(I:C) HMW, another TLR3 ligand, showed a similar reduction in TNF $\alpha$  but a significant increase in IFN $\alpha$ 2 upon Siglec-7 crosslinking ([Supplementary Figures 1B, C](#)). Although *cis*-ligands typically mask Siglec-7 and impair downstream signaling (42), removal of cell surface glycans with sialidase did not abolish QA79's inhibitory activity. QA79 maintained a significant inhibitory effect on Poly(I:C) LMW-induced TNF $\alpha$  production following sialidase treatment ([Figure 1B](#)). However, QA79 showed only a trending reduction of IFN $\alpha$ 2 compared to IgG control after sialidase treatment ([Figure 1C](#)). We observed reduced IFN $\alpha$ 2 baseline levels in the IgG control group after sialidase treatment compared to non-sialidase treated samples, which may account for the non-significant difference in IFN $\alpha$ 2 between QA79 and IgG control conditions after sialidase treatment ([Figure 1C](#)). These findings suggest that QA79 is a stronger agonist antibody than S7.7 after F(ab')<sub>2</sub> crosslinking for Siglec-7-mediated inhibition of TLR3 activation.

Next, we investigated whether Siglec-7 crosslinking could inhibit TNF $\alpha$  produced from other TLRs. Crosslinking Siglec-7 with QA79 did not significantly reduce TLR4-induced TNF $\alpha$  after LPS treatment ([Supplementary Figure 1D](#)). However, crosslinking Siglec-7 and activating TLR7 and TLR8 with R848 significantly reduced TNF $\alpha$  ([Supplementary Figures 1E, F](#)). This data showed that crosslinking Siglec-7 with QA79 inhibited endosomal TLR-mediated TNF $\alpha$  production, with the greatest effectiveness against TLR3.

### Antibody engagement induced rapid internalization of Siglec-7

It is understood that inhibitory receptors need to co-localize with activation receptors to inhibit downstream signaling (43). We studied whether cell surface Siglec-7 becomes internalized upon antibody engagement to enable possible co-localization with TLR3. U937 cells were preincubated with QA79 and Siglec-7 surface levels were assessed with a fluorescent secondary antibody. Within approximately 8 minutes, 50% of surface expressed Siglec-7 was internalized ([Figures 1D–F](#)). After the initial rapid decrease in surface Siglec-7, the amount of surface Siglec-7 steadily reduced over the remaining 3 hours; although at a diminished rate ([Figures 1D–F](#)).

Since the rapid internalization of Siglec-7 was induced by antibody engagement, we wanted to investigate whether the internalization was Siglec-7 specific or a Fc $\gamma$ R-mediated uptake process. To distinguish between these possibilities, we performed an internalization experiment using Fc block prior to QA79 incubation. Fc blockade showed no impact on Siglec-7 internalization after either 5 or 30 minute QA79 treatment compared to non-Fc block treated cells ([Figures 1G, H](#)), confirming that the observed internalization of Siglec-7 reflects Siglec-7-specific trafficking rather than non-specific Fc $\gamma$ R-mediated uptake.

Following receptor internalization, proteins are either recycled or trafficked to endolysosome for degradation (44). To determine the fate of Siglec-7 after internalization, immunoblot analysis was performed. This revealed a significant decrease in total Siglec-7 within 30 minutes of QA79 treatment compared to IgG control ([Figures 1I, J](#)). This rapid reduction suggests that internalized Siglec-7 undergoes degradation rather than recycling, consistent with a previous QA79-induced degradation study in Ba/F3 overexpression cells (45). Collectively, these findings establish QA79-mediated crosslinking triggers rapid Fc $\gamma$ R-independent internalization of surface Siglec-7, providing a mechanistic basis for the reduction in TLR3-induced TNF $\alpha$  in U937 cells.

### Crosslinking Siglec-7 decreased TLR3-mediated TNF $\alpha$ from primary monocytes and macrophages

Cell lines have distinct immune responses and cytokine profiles compared to primary immune cells due to altered signaling components (46–49). To validate our U937 cell findings in primary cells, we first characterized Siglec-7 expression across human peripheral blood immune cells. Analysis revealed high Siglec-7 expression, at both mRNA and protein levels, on myeloid and NK cell populations ([Figures 2A, B](#); [Supplementary Figure 2](#)). Functionally, QA79-mediated Siglec-7 crosslinking on both monocytes and macrophages reduced TNF $\alpha$  following Poly(I:C) LMW stimulation, while effects on IFN $\alpha$ 2 and other pro-inflammatory cytokines were not significantly changed ([Figures 2C–F](#); [Supplementary Figures 3A, B](#)). Additionally, both monocytes and macrophages exhibited rapid internalization of surface Siglec-7 within 5 minutes of QA79 treatment ([Figures 2G,](#)

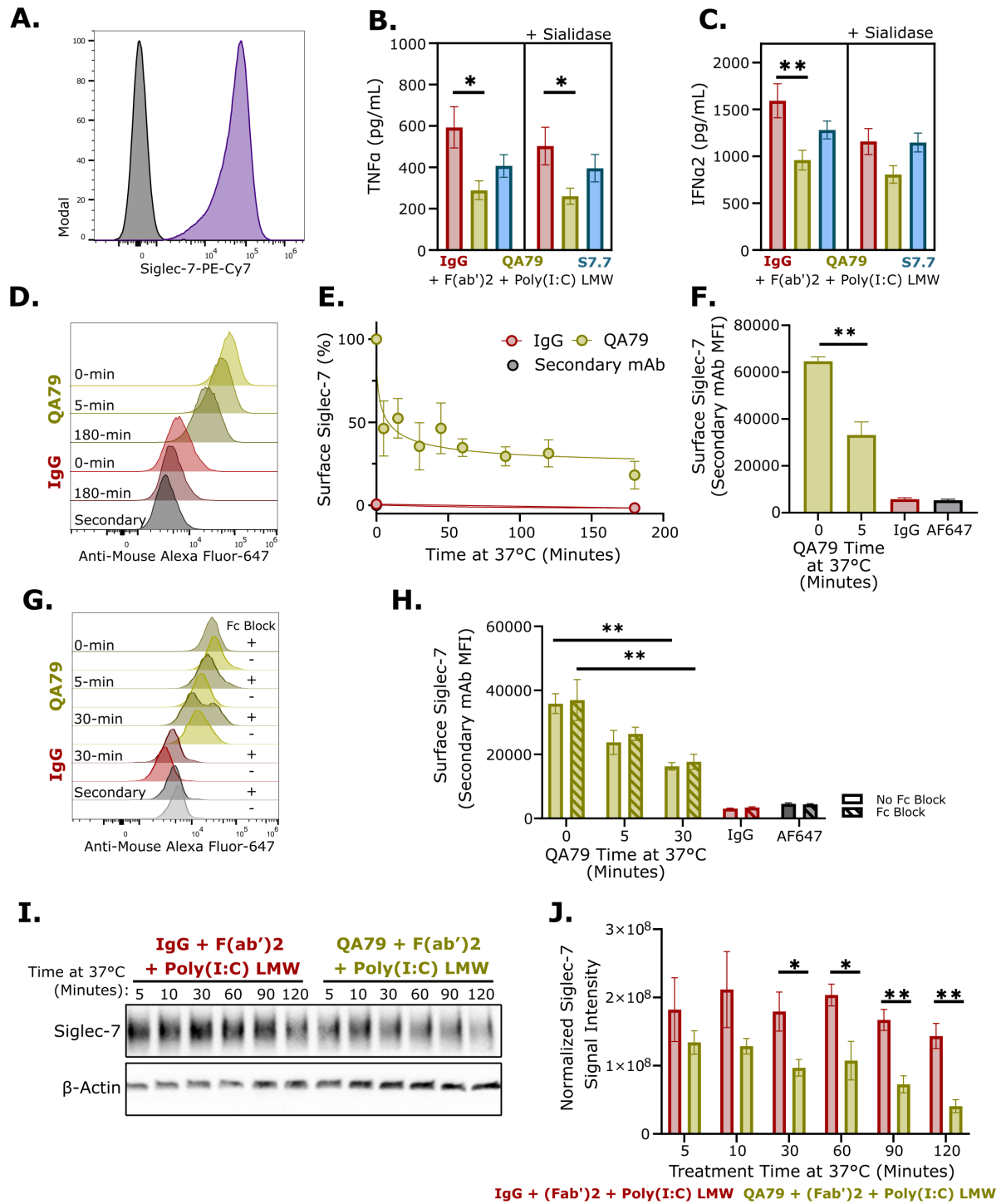


FIGURE 1

Siglec-7 agonism reduced TLR3-induced pro-inflammatory cytokines and induced rapid internalization of Siglec-7. (A) Representative flow cytometry histogram of Siglec-7 staining on U937 cells. Black: Isotype, Purple: Siglec-7 (n=3). TNFα (B) or IFNα2 (C) ELISA from baseline or 125 μM sialidase treated U937 cells preincubated with 10 μg/mL IgG or QA79 for 30 minutes on ice prior to treating with 2 μg/mL F(ab')2 and 1.25 μg/mL Poly(I:C) LMW for 24 hours. Data are mean ± SEM, and statistics are a One-Way ANOVA with Tukey's multiple comparison test; \*p<0.05, \*\*p<0.01 (n=4 experiments ran in triplicate). (D) Representative histogram of anti-mouse Alexa Fluor-647 staining of U937 cells preincubated with 5 μg/mL IgG or QA79 for 30 minutes on ice prior to incubating at 37 °C for the indicated times. Normalized quantification to time=0 (E) or Raw MFI values (F) from panel (D) Data are mean ± SEM, and statistics are a student's T-test; \*\*p<0.01. (n=2 experiments ran in duplicate). (G) Representative histogram or (H) raw MFI values of anti-mouse Alexa Fluor-647 staining of U937 cells, with or without Fc block, followed by incubated with 5 μg/mL IgG or QA79 for 30 minutes on ice before incubating at 37 °C for the indicated times. Data are mean ± SEM, and statistics are a student's T-test; \*\*p<0.01. (n=2 experiments ran in duplicate). Representative western blot (I) or normalized Siglec-7 signal intensity (J) of U937 cells preincubated with 25 μg/mL IgG or QA79 for 30 minutes on ice prior to incubating at 37 °C for the indicated times (in minutes) cotreated with 2 μg/mL F(ab')2 and 1.25 μg/mL Poly(I:C) LMW. Data are mean ± SEM, and statistics are a student's T-test; \*p<0.05, \*\*p<0.01 (n=4).

H). Together these data establish that rapid Siglec-7 internalization and inhibition of TLR3-mediated TNF $\alpha$  production is a conserved feature of myeloid cell biology.

Having confirmed rapid Siglec-7 internalization on primary myeloid cells, we next examined the longer-term fate of Siglec-7 following QA79 engagement. Analysis of Siglec-7 surface levels on macrophages 24 and 48 hours after QA79 treatment showed a persistent and significant reduction (Figure 2I). The prolonged reduction of surface Siglec-7 further supports Siglec-7 degradation upon internalization and suggests minimal recycling or *de novo* synthesis within 48 hours.

To further understand the pathways involved in QA79-mediated Siglec-7 internalization, we conducted a proteomic analysis. To induce robust downstream signaling events of Siglec-7, macrophages were treated for 3 hours with plate-bound QA79. Among all proteins in the dataset, Siglec-7 showed the most significant decrease while TLR3 remained unchanged (Figures 2J; Supplementary Table 2), consistent with our hypothesis of Siglec-7 specific degradation. Protein Set Enrichment analysis revealed QA79 treatment upregulated processes involved in multivesicular body sorting, viral budding, and lysosomal transport (Figures 2J; Supplementary Figure 3C). This was further confirmed by a significant upregulation of ESCRT pathway components: VPS4A, VPS4B, and VPS37A (Figure 2J). These findings suggest a pathway wherein Siglec-7 undergoes receptor-mediated endocytosis with endolysosomal trafficking and degradation. Collectively, our results provided mechanistic insights into the antibody induced internalization of Siglec-7 and demonstrated that QA79-mediated crosslinking of Siglec-7 reduced TLR3-induced TNF $\alpha$  in both primary monocytes and macrophages.

## Siglec-7 is trafficked to the endolysosome after rapid internalization

We hypothesized that rapid internalization of surface Siglec-7 facilitates endolysosomal trafficking and subsequent co-localization with TLR3, leading to the reduction in TLR3-mediated TNF $\alpha$ . We used image-based flow cytometry to assess time-dependent Siglec-7 co-localization with TLR3, Rab7a (late endosome marker), and LAMP1 (lysosome marker) in QA79-treated U937 cells (Figure 3A). Profiling cell masks generated by the IDEAs software, approximately 50% of Siglec-7 is lost from both cell surface and internal cell masks following QA79 treatment and Poly(I:C) LMW stimulation (Figures 3B, C). The images also revealed distinct time-dependent dynamics of Siglec-7 trafficking. Within 5–10 minutes, internalized Siglec-7 rapidly co-localized with Rab7a and LAMP1-positive endolysosome with minimal TLR3 overlap (Figure 3A). By 15–30 minutes, TLR3 was recruited to Siglec-7 positive endolysosomes with a peak co-localization between Siglec-7 and TLR3 occurring at 30 minutes (Figures 3A, D). Interestingly, co-localization between Siglec-7, TLR3, and LAMP1 did not induce TLR3 degradation (Figure 3A).

Next, we evaluated if the co-localization between internalized Siglec-7 and TLR3 is dependent on Poly(I:C) LMW. After 30 minutes of QA79 treatment, there was a comparable reduction of internalized Siglec-7 intensity with or without Poly(I:C) LMW

(Figures 3E, F). Furthermore, the co-localization of internalized Siglec-7 with TLR3 was similar with or without Poly(I:C) LMW (Figures 3E, G). Our data demonstrated that upon antibody engagement, Siglec-7 undergoes rapid endolysosome trafficking, during which it co-localized with TLR3 through a mechanism independent of TLR3 ligand presence.

## Siglec-7 crosslinking inhibited TLR3-mediated NF- $\kappa$ B phosphorylation

TLR3 promotes pro-inflammatory cytokine production primarily through NF- $\kappa$ B activation (2). We next studied whether the co-localization of internalized Siglec-7 with TLR3 after QA79 treatment reduced TLR3-induced NF- $\kappa$ B phosphorylation in U937 cells. Crosslinking Siglec-7 with QA79 decreased NF- $\kappa$ B phosphorylation relative to total NF- $\kappa$ B after Poly(I:C) LMW stimulation with a peak reduction occurring after 30 minutes (Figures 4A, B). However, by 60 to 90 minutes the ratio of phosphorylated NF- $\kappa$ B to total NF- $\kappa$ B was not significantly changed between IgG isotype control and QA79 samples (Figures 4A, B). This suggests that the loss of Siglec-7 inhibitory function potentially enables restoration of phosphorylated NF- $\kappa$ B at later timepoints.

Collectively, these time-dependent dynamics support a model whereby selective Siglec-7 degradation diminished its inhibitory capacity against TLR3 activation, thereby permitting restoration of TLR3-mediated NF- $\kappa$ B signaling. Overall, QA79-mediated Siglec-7 crosslinking suppressed NF- $\kappa$ B phosphorylation following TLR3 activation, potentially contributing to the diminished TNF $\alpha$  response in U937 cells, monocytes, and macrophages. (Figure 4C).

## Discussion

The Siglec family of immune checkpoint receptors play critical roles in maintaining tissue homeostasis with disruption of their regulatory function being implicated in the pathogenesis of multiple disease conditions (50, 51). It is evident that Siglec-7 can play key roles in both oncology and immune-mediated inflammatory disorders. In oncology, Siglec-7 function is widely characterized in multiple tumor microenvironments, particularly with respect to NK cell activity (52–54). Preclinical oncology models show that antibody-mediated antagonism or degradation of Siglec-7 promoted NK cell-mediated cytotoxicity leading to reduced tumor growth and increased survival of Siglec-7 antibody-treated mice in those studies (55–57). Conversely, dysregulated Siglec-7 has been implicated in relapsing-remitting Multiple Sclerosis, Type-2 Diabetes, and solid organ transplant rejection (27–29). *In vitro*, QA79 antibody-mediated Siglec-7 crosslinking reduced GM-CSF-induced eosinophil activation and IgE-mediated activation of mast cells and basophils (30–32). In this study, we are the first to show that QA79 antibody-mediated crosslinking of Siglec-7 and not S7.7 significantly inhibited TLR3-induced TNF $\alpha$  in U937 cells (Figure 1B), monocytes (Figure 2C), and macrophages (Figure 2E) compared to other activated TLRs (Supplementary

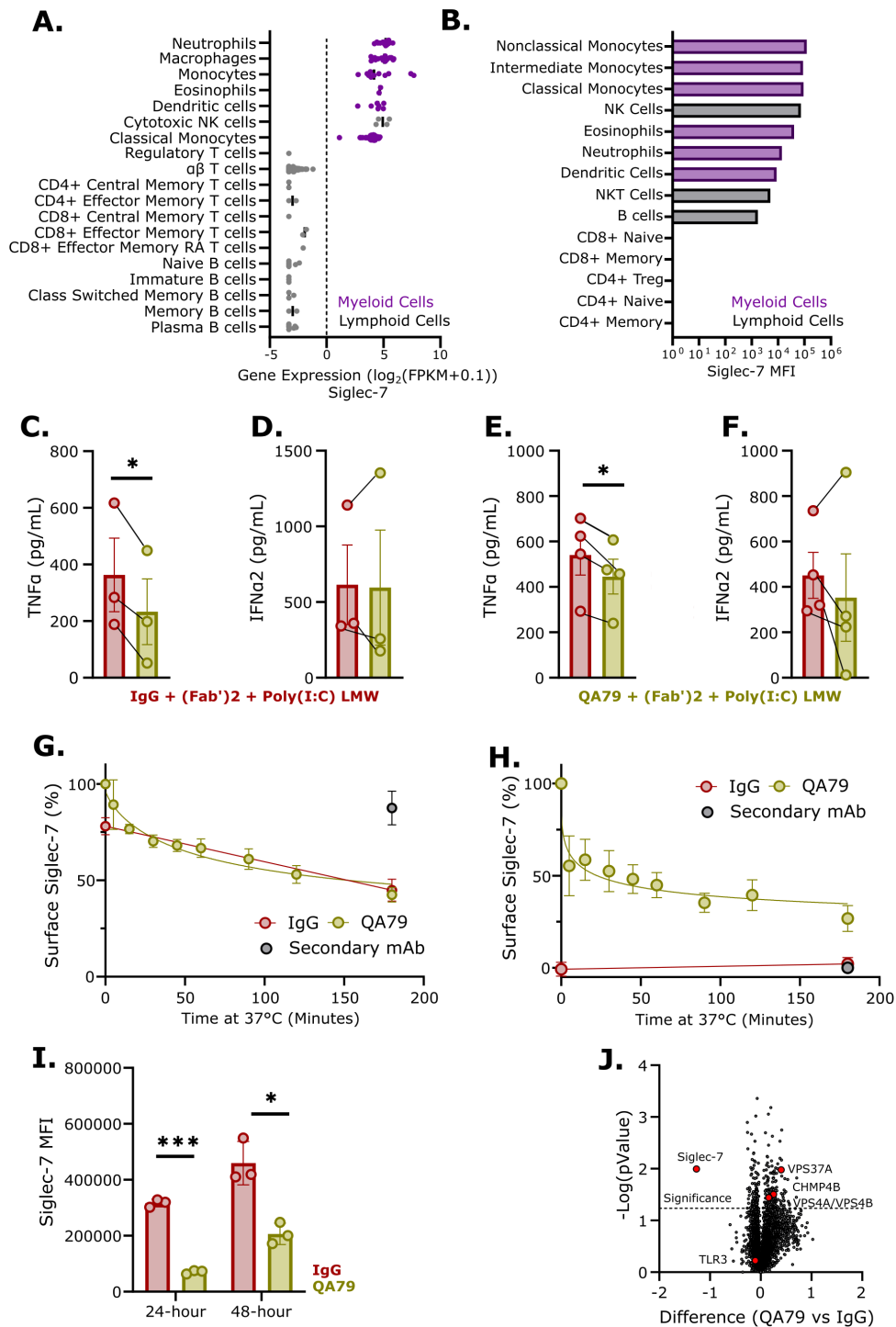


FIGURE 2

Agonism of Siglec-7 decreased TLR3-mediated TNF $\alpha$  in primary monocytes and macrophages. **(A)** Relative Siglec-7 mRNA expression in human blood immune cells (BLUEPRINT data set). **(B)** Representative Siglec-7 MFI of whole blood immunophenotyping (n=2). TNF $\alpha$  **(C)** or IFN $\alpha$ 2 **(D)** ELISA from primary human monocytes preincubated with 20  $\mu$ g/mL IgG or QA79 for 30-minutes on ice before treating with 2  $\mu$ g/mL F(ab')<sub>2</sub> and 1.25  $\mu$ g/mL Poly(I:C) LMW for 24-hours. Data are mean  $\pm$  SEM, and statistics are a student's T-test; \*p<0.05 (n=3 donors). TNF $\alpha$  **(E)** or IFN $\alpha$ 2 **(F)** ELISA from primary human macrophages preincubated with 20  $\mu$ g/mL IgG or QA79 for 30 minutes on ice before treating with 2  $\mu$ g/mL F(ab')<sub>2</sub> and 1.25  $\mu$ g/mL Poly(I:C) LMW for 24 hours. Data are mean  $\pm$  SEM, and statistics are a student's T-test; \*p<0.05 (n=3 donors). Normalized quantification to time=0 of the anti-mouse Alexa Fluor-647 secondary to detect surface levels of Siglec-7 on primary human monocytes **(G)** or primary human macrophages **(H)** post incubation at 37 °C with 5  $\mu$ g/mL IgG or QA79. (n=3 donors). **(I)** Flow cytometry profiling of Siglec-7 on primary macrophages after treatment at 37 °C with 5  $\mu$ g/mL IgG or QA79 for the indicated timepoints. Data are mean  $\pm$  SEM, and statistics are a student's T-test; \*p<0.05, \*\*\*p<0.001 (n=3 donors). **(J)** Volcano plot showing differential total protein abundance in primary macrophages stimulated for 3 hours at 37 °C on plates coated with 15  $\mu$ g/mL IgG or QA79. (n=3 donors).

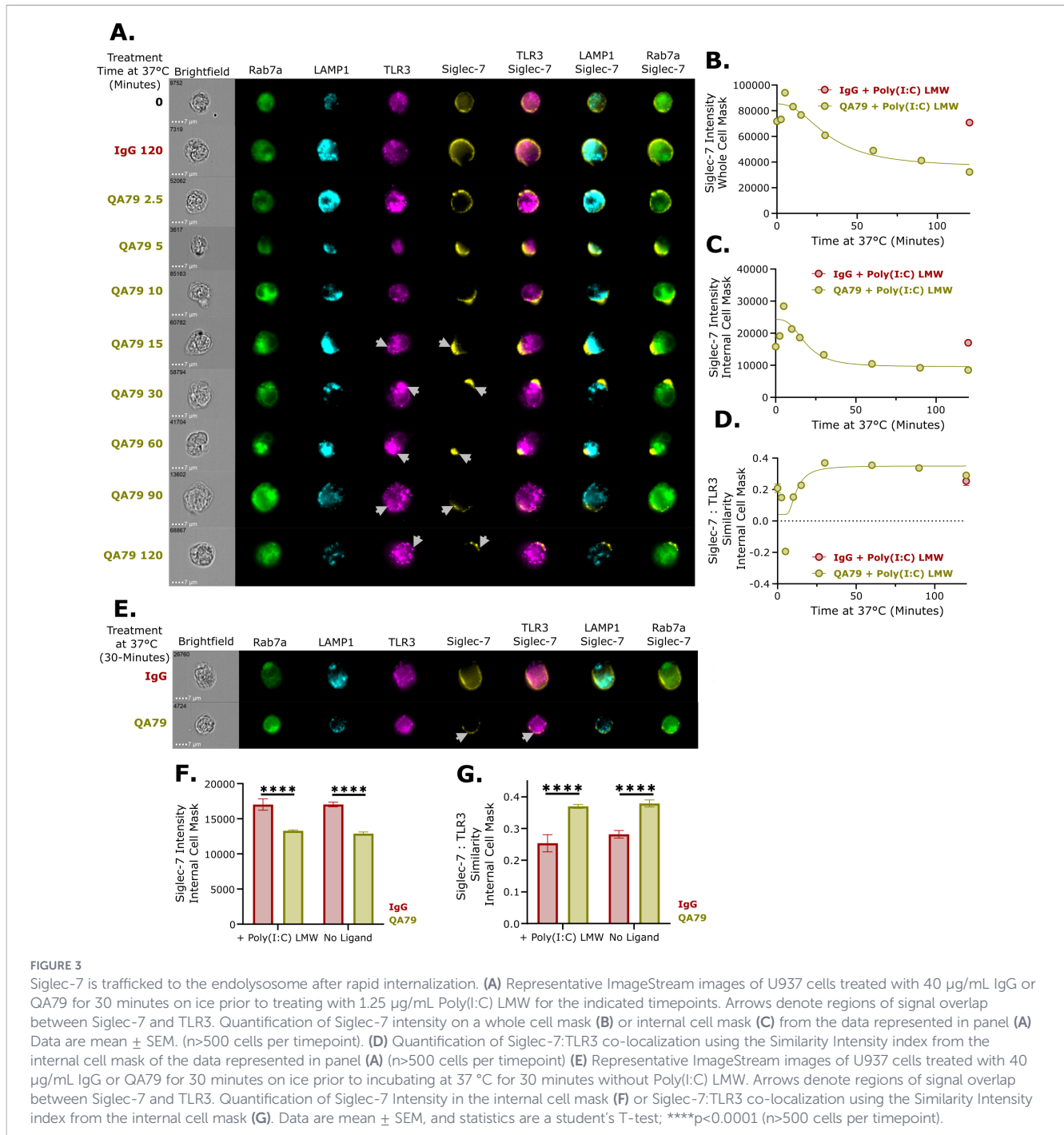


FIGURE 3

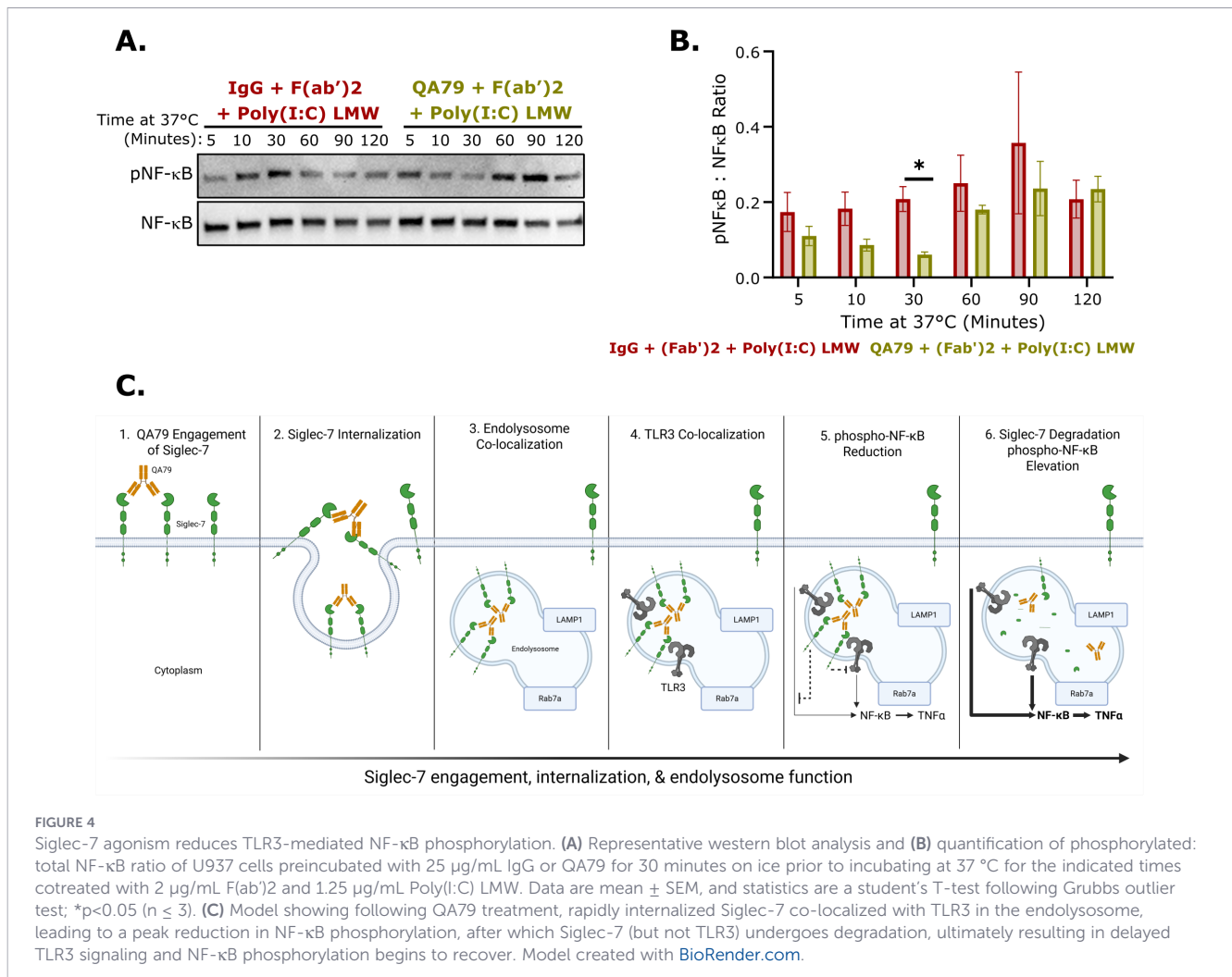
Siglec-7 is trafficked to the endolysosome after rapid internalization. (A) Representative ImageStream images of U937 cells treated with 40  $\mu\text{g}/\text{mL}$  IgG or QA79 for 30 minutes on ice prior to treating with 1.25  $\mu\text{g}/\text{mL}$  Poly(I:C) LMW for the indicated timepoints. Arrows denote regions of signal overlap between Siglec-7 and TLR3. Quantification of Siglec-7 intensity on a whole cell mask (B) or internal cell mask (C) from the data represented in panel (A). Data are mean  $\pm$  SEM. ( $n > 500$  cells per timepoint). (D) Quantification of Siglec-7:TLR3 co-localization using the Similarity Intensity index from the internal cell mask of the data represented in panel (A) ( $n > 500$  cells per timepoint). (E) Representative ImageStream images of U937 cells treated with 40  $\mu\text{g}/\text{mL}$  IgG or QA79 for 30 minutes on ice prior to incubating at 37°C for 30 minutes without Poly(I:C) LMW. Arrows denote regions of signal overlap between Siglec-7 and TLR3. Quantification of Siglec-7 Intensity in the internal cell mask (F) or Siglec-7:TLR3 co-localization using the Similarity Intensity index from the internal cell mask (G). Data are mean  $\pm$  SEM, and statistics are a student's T-test; \*\*\*\* $p < 0.0001$  ( $n > 500$  cells per timepoint).

Figure 1). We also observed reduced NF- $\kappa\text{B}$  phosphorylation (Figures 4A, B) following the rapid internalization and endolysosomal trafficking of Siglec-7 where it co-localized with TLR3 (Figure 3D).

Protein glycosylation plays critical roles in immune regulation and diminished glycosylation can accelerate autoimmune disease progression (58). Glycan-recognizing receptors require intact ligand-bound glycan structures to initiate bidirectional signaling. Several Siglecs bind to and negatively regulate TLR4-mediated activity (3–9). When sialic acids were removed from TLR4, Siglec-E could no longer bind TLR4 or recruit the inhibitory phosphatases SHP-1 and SHP-2 to suppress TLR4 activation,

resulting in enhanced pro-inflammatory cytokine production (7, 59). Disrupting the Siglec-TLR regulatory network may cause or enhance pathological conditions. Future studies should evaluate whether abnormal TLR3 glycosylation could affect the interaction with Siglec-7, potentially dysregulating inflammation-mediated immune responses.

Our study demonstrated that Siglec-7 performs distinct functions depending on its cellular localization. At the cell surface, myeloid-expressed Siglec-7 binds *in trans* to CD43 expressed on T cells (24–26). This Siglec-7:CD43 interaction reduced T cell proliferation and skewed cells toward Th2 cytokine production (26). Supporting this cell surface immunosuppressive



role, antibody-mediated antagonism of Siglec-7 (clone S7.7) in mixed leukocyte reactions enhanced Th1 cytokine production and, separately, promoted NK cell-mediated killing of Raji B cells (26, 40). However, Siglec-7 engagement by QA79 on myeloid cells triggered rapid FcγR-independent internalization (Figures 1D–H) and endolysosomal trafficking of Siglec-7 (Figure 3). While other Siglecs also undergo internalization and endolysosomal trafficking (37, 60–62), our study discovered an unexpectedly rapid antibody-mediated internalization rate of Siglec-7 (clone QA79) on monocytes and macrophages (Figures 2G, H). This resembles mouse Siglec-F, another CD33-related Siglec that is internalized independently of clathrin and dynamin and is rapidly trafficked to lysosomes (62). Once Siglec-7 localized to the endolysosome (Figure 3), TLR3-mediated TNFα production (Figure 1B) and NF-κB phosphorylation was reduced (Figure 4). Our data suggests Siglec-7 also inhibits TLR7 and TLR8-mediated TNFα production, though with somewhat lower potency (Supplementary Figure 1E). Additional studies should examine if myeloid cells internalize Siglec-7 during immune-mediated inflammatory conditions and how Siglec-7 internalization affects TLR3 signaling.

TLR3 activation produces both pro-inflammatory cytokines and type-1 interferons (2). As such, we also evaluated IFNα2 production following TLR3 activation. While TLR3-mediated

TNFα was consistently reduced following QA79 antibody-mediated Siglec-7 crosslinking, IFNα2 reduction was only significantly reduced from U937 cells (Figure 1C) as compared to monocytes (Figure 2D) and macrophages (Figure 2F). This difference likely reflects inherent immune regulatory mechanisms between myeloid cell lines and primary cells (46–49). The differential regulation of TNFα versus IFNα2 by Siglec-7 following QA79 antibody treatment suggests a possible selective mechanism whereby Siglec-7 agonism preferentially inhibits certain specific TLR3 downstream adaptor proteins (63). This selectivity may explain why QA79 crosslinking on U937 cells decreased IFNα2 after TLR3 activation (Figure 1C) but slightly increased IFNα2 after TLR7 and TLR8 activation (Supplementary Figure 1F) (63). Future mechanistic studies should examine how Siglec-7 crosslinking affects TLR3 downstream adaptor protein recruitment and activation in primary cells.

Most clinical stage immune checkpoint receptor agonist antibodies (e.g., anti-PD1, Peresolimab, Rosnilimab, and anti-BTLA, Venanprubart) target T and B cells (64, 65), yet myeloid-directed approaches may offer advantages in pathologies where myeloid inflammation drives T cell activation. Our data indicates that Siglec-7 may have unexplored therapeutic potential in pathologies driven by TLR3-mediated myeloid dysfunction, such as

solid organ transplant rejection. During early allograft rejection, myeloid cells initially infiltrate the transplanted organ and subsequently promote organ recipient T cell migration and activation (29, 66, 67). TLR3 exhibits aberrant activation during acute transplant rejection, while TLR3 knockout mice demonstrate prolonged allograft survival compared to wild-type controls (68–71). Notably, recent clinical findings linked elevated Siglec-7 expression with improved allograft survival (29), suggesting that Siglec-7-mediated regulation of myeloid activation may be protective in this context. Conversely, elevated CD43 expression on CD8+ T cells was associated with decreased allograft survival (72), and inflammation-induced glycan shedding from T cells may disrupt the Siglec-7:CD43 interaction, thereby amplifying inflammatory responses (26, 73).

Autoimmune diseases, like Systemic Lupus Erythematosus (SLE), are also characterized by myeloid dysfunction driven by chronic endosomal TLR activation. In SLE, this stems from anti-nucleic acid autoantibodies forming immune complexes that facilitate self-nucleic acid endosomal uptake and increased type-1 interferon production (74, 75). Supporting a protective role for Siglec-7 in SLE, Siglec-E knockout mice developed SLE-like phenotypes including increased autoantibodies, immune complex deposition, and renal pathology (75). Future studies should investigate the therapeutic potential of targeting Siglec-7 and disrupting TLR3 function in SLE. Collectively, these findings suggest that antibody-mediated Siglec-7 agonism represents a promising strategy to suppress myeloid cell activation during inflammation-driven pathologies, thereby preventing subsequent T cell activation and restoring immune homeostasis.

In conclusion, our results suggest Siglec-7 has unique endolysosome functions. After screening multiple TLRs, we show that Siglec-7 has a previously unrecognized role as an inhibitory receptor for TLR3 in primary human monocytes and macrophages. We demonstrate that Siglec-7 reduced TLR3-mediated TNF $\alpha$  production and NF- $\kappa$ B phosphorylation after treatment with F(ab')<sub>2</sub> crosslinked antibody clone QA79. Moreover, this novel finding provides a strong rationale for future analysis of Siglec-7 function in autoimmune disease conditions and further investigation of whether Siglec-7 agonism can be beneficial to re-balance cellular pathologies caused by aberrant TLR3 signaling.

## Data availability statement

The proteomic data have been deposited in Proteome Xchange and jPost Repository under accession numbers PXD075217 - <https://proteomecentral.proteomexchange.org/ui?pxid=PXID075217> and JPST004448 - <https://repository.jpostdb.org/entry/JPST004448>.

## Ethics statement

The studies involving humans were approved by Sanofi Bioethics Committee (BEC). The studies were conducted in accordance with the

local legislation and institutional requirements. The human samples used in this study were acquired from Research Blood Components (RBC, Boston, MA) and the Sanofi Donor Research Program (Boston, MA). The participants provided their written informed consent to participate in this study.

## Author contributions

JK: Writing – original draft, Writing – review & editing, Formal analysis, Visualization, Methodology, Validation, Investigation, Conceptualization. JS: Formal analysis, Investigation, Writing – review & editing. BY: Writing – review & editing, Investigation, Formal analysis. HW: Formal analysis, Software, Investigation, Writing – review & editing. BZ: Writing – review & editing, Supervision, Project administration. AM: Project administration, Conceptualization, Supervision, Writing – original draft. SH: Supervision, Conceptualization, Writing – original draft, Project administration. GW: Conceptualization, Writing – original draft, Project administration, Supervision.

## Funding

The author(s) declared that financial support was received for this work and/or its publication. Funding of this work was sponsored by Sanofi.

## Acknowledgments

We thank Alexandra Hicks for her guidance and critical review of the manuscript.

## Conflict of interest

The authors were employees of Sanofi when this work was performed.

## Generative AI statement

The author(s) declared that generative AI was used in the creation of this manuscript. Limited use of a Generative AI tool was used for manuscript editing.

Any alternative text (alt text) provided alongside figures in this article has been generated by Frontiers with the support of artificial intelligence and reasonable efforts have been made to ensure accuracy, including review by the authors wherever possible. If you identify any issues, please contact us.

## Publisher's note

All claims expressed in this article are solely those of the authors and do not necessarily represent those of their affiliated organizations, or those of the publisher, the editors and the reviewers. Any product that may be evaluated in this article, or claim that may be made by its manufacturer, is not guaranteed or endorsed by the publisher.

## Supplementary material

The Supplementary Material for this article can be found online at: <https://www.frontiersin.org/articles/10.3389/fimmu.2026.1764343/full#supplementary-material>

### SUPPLEMENTARY FIGURE 1

Siglec-7 agonism of U937 cells inhibits proinflammatory cytokines from endosomal TLRs. (A) Representative flow cytometry histogram of TLR3 staining in U937 cells. Black: Isotype, Purple: TLR3 (n=2). TNF $\alpha$  (B) or IFN $\alpha$ 2

(C) ELISA from U937 cells preincubated with 10  $\mu$ g/mL IgG or QA79 for 30 minutes on ice prior to treating with 2  $\mu$ g/mL F(ab')<sub>2</sub> and 1.25  $\mu$ g/mL Poly(I:C) HMW for 24 hours. Data are mean  $\pm$  SEM, and statistics are a Student T-test; \*p<0.05 (n=3 experiments ran in triplicate). (D) TNF $\alpha$  ELISA from U937 cells preincubated with 10  $\mu$ g/mL IgG or QA79 for 30 minutes on ice prior to treating with 2  $\mu$ g/mL F(ab')<sub>2</sub> and 2 ng/mL LPS for 24 hours. Data are mean  $\pm$  SEM, and statistics are a Student T-test (n=2 experiments ran in triplicate). TNF $\alpha$  (E) or IFN $\alpha$ 2 (F) ELISA from U937 cells preincubated with 10  $\mu$ g/mL IgG or QA79 for 30 minutes on ice prior to treating with 2  $\mu$ g/mL F(ab')<sub>2</sub> and 2.5  $\mu$ g/mL R848 for 24 hours. Data are mean  $\pm$  SEM, and statistics are a Student T-test; \*p<0.05 (n=3 experiments ran in triplicate).

### SUPPLEMENTARY FIGURE 2

Gating strategy of human whole blood Siglec-7 immunophenotyping.

### SUPPLEMENTARY FIGURE 3

Siglec-7 agonism induced minimal cytokine changes in primary cells. MSD multiplex assay profiling additional cytokines known to be downstream of TLR3 activation from primary human monocytes (A) or primary human macrophages (B) preincubated with 20  $\mu$ g/mL IgG or QA79 for 30 minutes on ice prior to treating with 2  $\mu$ g/mL F(ab')<sub>2</sub> and 1.25  $\mu$ g/mL Poly(I:C) LMW for 24 hours. (n=1 donor ran in triplicate). (C) Protein Set Enrichment analysis of proteins significantly altered by a 3 hour stimulation with plate bound QA79 compared to IgG control in primary macrophages. (n=3 donors).

## References

- Hosseini AM, Majidi J, Baradaran B, Yousefi M. Toll-like receptors in the pathogenesis of autoimmune diseases. *Adv Pharm Bull.* (2014) 5:605–14. doi: 10.1517/apb.2015.082
- Hsieh ML, Nishizaki D, Adashek JJ, Kato S, Kurzrock R. Toll-like receptor 3: a double-edged sword. *Biomark Res.* (2025) 13:32. doi: 10.1186/s40364-025-00739-5
- Yang D, Wu Y, Chen G-Y. Regulation of the immune response by Siglec-1 through phosphorylation of Src at Ser17. *J Immunol.* (2020) 204:68.5–5. doi: 10.4049/jimmunol.204.supp.68.5
- Yang D, Wu Y, Chen G-Y. Siglec-1 negatively regulates TLR4-mediated inflammatory response by uniquely controlling Src phosphorylation at Ser17. *J Immunol.* (2019) 202:64.17–7. doi: 10.4049/jimmunol.202.supp.64.17
- Ishida A, Akita K, Mori Y, Tanida S, Toda M, Inoue M, et al. Negative regulation of toll-like receptor-4 signaling through the binding of glycosylphosphatidylinositol-anchored glycoprotein, CD14, with the sialic acid-binding lectin, CD33\*. *J Biol Chem.* (2014) 289:25341–50. doi: 10.1074/jbc.m113.523480
- Wu Y, Ren D, Chen G-Y. Siglec-E negatively regulates the activation of TLR4 by controlling its endocytosis. *J Immunol.* (2016) 197:3336–47. doi: 10.4049/jimmunol.1600772
- Karmakar J, Mandal C. Interplay between sialic acids, siglec-E, and neu1 regulates myD88- and TRIF-dependent pathways for TLR4-activation during leishmania donovani infection. *Front Immunol.* (2021) 12:626110. doi: 10.3389/fimmu.2021.626110
- Spence S, Greene MK, Fay F, Hams E, Saunders SP, Hamid U, et al. Targeting Siglecs with a sialic acid-decorated nanoparticle abrogates inflammation. *Sci Transl Med.* (2015) 7:303ra140. doi: 10.1126/scitranslmed.aab3459
- Råberg L, Jia F, von Mentzer U, Venkatakrishnan V, Karlsson NG, Stubelius A. Sialoglycans modulate Siglec-5-TLR4 interactions in osteoarthritis. *iScience.* (2025) 28:113979. doi: 10.1016/j.isci.2025.113979
- Reily C, Stewart TJ, Renfrow MB, Novak J. Glycosylation in health and disease. *Nat Rev Nephrol.* (2019) 15:346–66. doi: 10.1038/s41581-019-0129-4
- Crocker PR, Paulson JC, Varki A. Siglecs and their roles in the immune system. *Nat Rev Immunol.* (2007) 7:255–66. doi: 10.1038/nri2056
- Chen G-Y, Brown NK, Wu W, Khedri Z, Yu H, Chen X, et al. Broad and direct interaction between TLR and Siglec families of pattern recognition receptors and its regulation by Neu1. *eLife.* (2014) 3:e04066. doi: 10.7554/eLife.04066
- Nicoll G, Ni J, Liu D, Klenerman P, Munday J, Dubock S, et al. Identification and characterization of a novel siglec, siglec-7, expressed by human natural killer cells and monocytes\*. *J Biol Chem.* (1999) 274:34089–95. doi: 10.1074/jbc.274.48.34089
- Büll C, Nason R, Sun L, Coillie JV, Sørensen DM, Moons SJ, et al. Probing the binding specificities of human Siglecs by cell-based glycan arrays. *Proc Natl Acad Sci.* (2021) 118:e2026102118. doi: 10.1073/pnas.2026102118
- Carluccio CD, Padilla-Cortés L, Tiemblo-Martin M, Gheorghita GR, Oliva R, Cerofolini L, et al. Insights into siglec-7 binding to gangliosides: NMR protein assignment and the impact of ligand flexibility. *Adv Sci.* (2025) 12:2415782. doi: 10.1002/advs.202415782
- Crocker PR, Blixt O, Collins BE, van den Nieuwenhof IM, Paulson JC. Sialoside specificity of the siglec family assessed using novel multivalent probes IDENTIFICATION OF POTENT INHIBITORS OF MYELIN-ASSOCIATED GLYCOPROTEIN\*. *J Biol Chem.* (2003) 278:31007–19. doi: 10.1074/jbc.m304331200
- Yamaji T, Teranishi T, Alphey MS, Crocker PR, Hashimoto Y. A small region of the natural killer cell receptor, siglec-7, is responsible for its preferred binding to  $\alpha$ 2,8-disialyl and branched  $\alpha$ 2,6-sialyl residues A COMPARISON WITH siglec-9\*. *J Biol Chem.* (2002) 277:6324–32. doi: 10.1074/jbc.m110146200
- Avril T, Wagner ER, Willison HJ, Crocker PR. Sialic acid-binding immunoglobulin-like lectin 7 mediates selective recognition of sialylated glycans expressed on campylobacter jejuni lipooligosaccharides. *Infect Immun.* (2006) 74:4133–41. doi: 10.1128/iai.02094-05
- Suenaga T, Mori Y, Suzutani T, Arase H. Regulation of Siglec-7-mediated varicella-zoster virus infection of primary monocytes by cis-ligands. *Biochem Biophys Res Commun.* (2022) 613:41–6. doi: 10.1016/j.bbrc.2022.04.111
- Suenaga T, Mori Y, Suzutani T, Arase H. Siglec-7 mediates varicella-zoster virus infection by associating with glycoprotein B. *Biochem Biophys Res Commun.* (2022) 607:67–72. doi: 10.1016/j.bbrc.2022.03.060
- Carluccio CD, Amor TG, Lenza MP, Masi AA, Abreu C, Longo V, et al. Molecular basis of siglec-7 recognition by neisseria meningitidis serogroup Y CPS: implications for immune evasion. *JACS Au.* (2025) 5:2257–69. doi: 10.1021/jacsau.5c00214
- Brunetta E, Fogli M, Varchetta S, Bozzo L, Hudspeth KL, Marcenaro E, et al. The decreased expression of Siglec-7 represents an early marker of dysfunctional natural killer-cell subsets associated with high levels of HIV-1 viremia. *Blood.* (2009) 114:3822–30. doi: 10.1182/blood-2009-06-226332
- Varchetta S, Brunetta E, Roberto A, Mikulak J, Hudspeth KL, Mondelli MU, et al. Engagement of siglec-7 receptor induces a pro-inflammatory response selectively in monocytes. *PLoS One.* (2012) 7:e45821. doi: 10.1371/journal.pone.0045821
- Wisnovsky S, Möckl L, Malaker SA, Pedram K, Hess GT, Riley NM, et al. Genome-wide CRISPR screens reveal a specific ligand for the glycan-binding immune checkpoint receptor Siglec-7. *Proc Natl Acad Sci.* (2021) 118:e2015024118. doi: 10.1073/pnas.2015024118
- Yoshimura A, Asahina Y, Chang L-Y, Angata T, Tanaka H, Kitajima K, et al. Identification and functional characterization of a Siglec-7 counter-receptor on K562 cells. *J Biol Chem.* (2021) 296:100477. doi: 10.1016/j.jbc.2021.100477
- Stewart N, Daly J, Drummond-Guy O, Krishnamoorthy V, Stark JC, Riley NM, et al. The glyco-immune checkpoint receptor Siglec-7 interacts with T-cell ligands and regulates T-cell activation. *J Biol Chem.* (2024) 300(2):105579. doi: 10.1016/j.jbc.2023.105579
- Malhotra S, Castelló J, Bustamante M, Vidal-Jordana A, Castro Z, Montalban X, et al. SIGLEC1 and SIGLEC7 expression in circulating monocytes of patients with multiple sclerosis. *Mult Scler J.* (2012) 19:524–31. doi: 10.1177/1352458512458718

28. Dharmadhikari G, Stolz K, Hauke M, Morgan NG, Varki A, de Koning E, et al. Siglec-7 restores  $\beta$ -cell function and survival and reduces inflammation in pancreatic islets from patients with diabetes. *Sci Rep.* (2017) 7:45319. doi: 10.1038/srep45319
29. Borges TJ, Lima K, Gassen RB, Liu K, Ganchiku Y, Ribas GT, et al. The inhibitory receptor Siglec-E controls antigen-presenting cell activation and T cell-mediated transplant rejection. *Sci Transl Med.* (2025) 17:eads2694. doi: 10.1126/scitranslmed.ads2694
30. Mizrahi S, Gibbs BF, Karra L, Ben-Zimra M, Levi-Schaffer F. Siglec-7 is an inhibitory receptor on human mast cells and basophils. *J Allergy Clin Immunol.* (2014) 134:230–233.e3. doi: 10.1016/j.jaci.2014.03.031
31. Legrand F, Landolina N, Zaffran I, Emeh RO, Chen E, Klion AD, et al. Siglec-7 on peripheral blood eosinophils: Surface expression and function. *Allergy.* (2019) 74:1257–65. doi: 10.1111/all.13730
32. Landolina N, Zaffran I, Smiljkovic D, Serrano-Candelas E, Schmiedel D, Friedman S, et al. Activation of Siglec-7 results in inhibition of *in vitro* and *in vivo* growth of human mast cell leukemia cells. *Pharmacol Res.* (2020) 158:104682. doi: 10.1016/j.phrs.2020.104682
33. Nakanishi M, Tamagawa-Mineoka R, Nishigaki H, Arakawa Y, Ohtsuka S, Katoh N. Role of siglec-E in MC903-induced atopic dermatitis. *Exp Dermatol.* (2025) 34:e70064. doi: 10.1111/exd.70064
34. Liu H, Zheng Y, Zhang Y, Li J, Fernandes SM, Zeng D, et al. Immunosuppressive Siglec-E ligands on mouse aorta are up-regulated by LPS via NF- $\kappa$ B pathway. *BioMed Pharmacother.* (2020) 122:109760. doi: 10.1016/j.biopha.2019.109760
35. Liu H, Li J, Wu N, She Y, Luo Y, Huang Y, et al. Supplementing glucose intake reverses the inflammation induced by a high-fat diet by increasing the expression of siglec-E ligands on erythrocytes. *Inflammation.* (2024) 47:609–25. doi: 10.1007/s10753-023-01932-0
36. Zeng Z, Li M, Wang M, Wu X, Li Q, Ning Q, et al. Increased expression of Siglec-9 in chronic obstructive pulmonary disease. *Sci Rep.* (2017) 7:10116. doi: 10.1038/s41598-017-09120-5
37. O'Sullivan JA, Carroll DJ, Cao Y, Salicru AN, Bochner BS. Leveraging Siglec-8 endocytic mechanisms to kill human eosinophils and Malignant mast cells. *J Allergy Clin Immunol.* (2018) 141:1774–1785.e7. doi: 10.1016/j.jaci.2017.06.028
38. Chen L, Patil S, Barbon J, Waire J, Laroux FS, McCarthy D, et al. Agonistic anti-DCIR antibody inhibits ITAM-mediated inflammatory signaling and promotes immune resolution. *JCI Insight.* (2024) 9:e176064. doi: 10.1172/jci.insight.176064
39. Hughes CS, Moggridge S, Müller T, Sorensen PH, Morin GB, Krijgsvelde J. Singlepot, solid-phase-enhanced sample preparation for proteomics experiments. *Nat Protoc.* (2019) 14:68–85. doi: 10.1038/s41596-018-0082-x
40. Hong S, Yu C, Rodrigues E, Shi Y, Chen H, Wang P, et al. Modulation of siglec-7 signaling via in situ-created high-affinity cis-ligands. *ACS Cent Sci.* (2021) 7:1338–46. doi: 10.1021/acscentsci.1c00064
41. Nicoll G, Avril T, Lock K, Furukawa K, Bovin N, Crocker PR. Ganglioside GD3 expression on target cells can modulate NK cell cytotoxicity via siglec-7-dependent and -independent mechanisms. *Eur J Immunol.* (2003) 33:1642–8. doi: 10.1002/eji.200323693
42. McCord KA, Wang C, Anhalt M, Poon WW, Gavin AL, Wu P, et al. Dissecting the ability of siglecs to antagonize  $\text{Fc}\gamma$  Receptors. *ACS Cent Sci.* (2024) 10:315–30. doi: 10.1021/acscentsci.3c00969
43. Pérez-Ferreros P, Gaus K, Goyette J. Tethered signaling in inhibitory immune receptors. *Front Phys.* (2019) 6:158. doi: 10.3389/fphy.2018.00158
44. Cullen PJ, Steinberg F. To degrade or not to degrade: mechanisms and significance of endocytic recycling. *Nat Rev Mol Cell Biol.* (2018) 19:679–96. doi: 10.1038/s41580-018-0053-7
45. Orr SJ, Morgan NM, Buick RJ, Boyd CR, Elliott J, Burrows JF, et al. SOCS3 targets siglec 7 for proteasomal degradation and blocks siglec 7-mediated responses\*. *J Biol Chem.* (2007) 282:3418–22. doi: 10.1074/jbc.c600216200
46. Kortmann J, Brubaker SW, Monack DM. Cutting edge: inflammasome activation in primary human macrophages is dependent on flagellin. *J Immunol.* (2015) 195:815–9. doi: 10.4049/jimmunol.1403100
47. Bagaev AV, Garaeva AY, Lebedeva ES, Pichugin AV, Ataulkhanov RI, Ataulkhanov FI. Elevated pre-activation basal level of nuclear NF- $\kappa$ B in native macrophages accelerates LPS-induced translocation of cytosolic NF- $\kappa$ B into the cell nucleus. *Sci Rep.* (2019) 9:4563. doi: 10.1038/s41598-018-36052-5
48. Sharif O, Bolshakov VN, Raines S, Newham P, Perkins ND. Transcriptional profiling of the LPS induced NF- $\kappa$ B response in macrophages. *BMC Immunol.* (2007) 8:1. doi: 10.1186/1471-2172-8-1
49. Şen B, Balci-Peynircioğlu B. Cellular models in autoinflammatory disease research. *Clin Transl Immunol.* (2024) 13:e1481. doi: 10.1002/cti2.1481
50. Brzezicka KA, Paulson JC. Impact of Siglecs on autoimmune diseases. *Mol Asp Med.* (2023) 90:101140. doi: 10.1016/j.mam.2022.101140
51. Macauley MS, Crocker PR, Paulson JC. Siglec-mediated regulation of immune cell function in disease. *Nat Rev Immunol.* (2014) 14:653–66. doi: 10.1038/nri3737
52. van Houtum EJ, Valk AH, Granado D, Lok J, van den Bogaard L, Remkes N, et al. Siglec-7 and Siglec-9 expression in primary triple negative and oestrogen receptor positive breast cancer and *in vitro* signalling. *Clin Transl Immunol.* (2024) 13:e1524. doi: 10.1002/cti2.1524
53. Benthani H, Zohair B, Rezouki I, Naji O, Miyara K, Ennachit S, et al. Elevated Siglec-7 expression correlates with adverse clinicopathological, immunological, and therapeutic response signatures in breast cancer patients. *Front Immunol.* (2025) 16:1573365. doi: 10.3389/fimmu.2025.1573365
54. Jiang K-Y, Qi L-L, Kang F-B, Wang L. The intriguing roles of Siglec family members in the tumor microenvironment. *biomark Res.* (2022) 10:22. doi: 10.1186/s40364-022-00369-1
55. Ibarlucea-Benitez I, Weitzenfeld P, Smith P, Ravetch JV. Siglecs-7/9 function as inhibitory immune checkpoints *in vivo* and can be targeted to enhance therapeutic antitumor immunity. *Proc Natl Acad Sci.* (2021) 118:e2107424118. doi: 10.1073/pnas.2107424118
56. Wang C, Hou Y, Zak J, Zheng Q, McCord KA, Wu M, et al. Reshaping the tumor microenvironment by degrading glycoimmune checkpoints Siglec-7 and -9. *BioRxiv.* (2024). doi: 10.1101/2024.10.11.617879. 2024.10.11.617879.
57. Bordoloi D, Kulkarni AJ, Adeniji OS, Pampena MB, Bhojnagarwala PS, Zhao S, et al. Siglec-7 glyco-immune binding mAbs or NK cell engager biologics induce potent antitumor immunity against ovarian cancers. *Sci Adv.* (2023) 9:eadh4379. doi: 10.1126/sciadv.adh4379
58. Szabó E, Faragó A, Bodor G, Gémes N, Puskás LG, Kovács L, et al. Identification of immune subsets with distinct lectin binding signatures using multi-parameter flow cytometry: correlations with disease activity in systemic lupus erythematosus. *Front Immunol.* (2024) 15:1380481. doi: 10.3389/fimmu.2024.1380481
59. Amith SR, Jayanth P, Franchuk S, Finlay T, Seyrantepe V, Beyaert R, et al. Neu1 desialylation of sialyl  $\alpha$ -2,3-linked  $\beta$ -galactosyl residues of TOLL-like receptor 4 is essential for receptor activation and cellular signaling. *Cell Signal.* (2010) 22:314–24. doi: 10.1016/j.cellsig.2009.09.038
60. Miralda I, Samanas NB, Seo AJ, Foronda JS, Sachen J, Hui Y, et al. Siglec-9 is an inhibitory receptor on human mast cells *in vitro*. *J Allergy Clin Immunol.* (2023) 152:711–724.e14. doi: 10.1016/j.jaci.2023.04.007
61. Shan D, Press OW. Constitutive endocytosis and degradation of CD22 by human B cells. *J Immunol (Baltim Md : 1950).* (1995) 154:4466–75. doi: 10.4049/jimmunol.154.9.4466
62. Tateno H, Li H, Schur MJ, Bovin N, Crocker PR, Wakarchuk WW, et al. Distinct endocytic mechanisms of CD22 (Siglec-2) and siglec-F reflect roles in cell signaling and innate immunity. *Mol Cell Biol.* (2007) 27:5699–710. doi: 10.1128/mcb.00383-07
63. Kawai T, Ikegawa M, Ori D, Akira S. Decoding Toll-like receptors: Recent insights and perspectives in innate immunity. *Immunity.* (2024) 57:649–73. doi: 10.1016/j.immuni.2024.03.004
64. Paluch C, Santos AM, Anzilotti C, Cornall RJ, Davis SJ. Immune checkpoints as therapeutic targets in autoimmunity. *Front Immunol.* (2018) 9:2306. doi: 10.3389/fimmu.2018.02306
65. Kuchroo JR, Goldman N, Sharpe AH. PD-1, BTLA and TIGIT as therapeutic targets for rheumatic disease. *Nat Rev Rheumatol.* (2026) 22, 89–104. doi: 10.1038/s41584-025-01296-9
66. Zhuang Q, Liu Q, Divito SJ, Zeng Q, Yatim KM, Hughes AD, et al. Graft-infiltrating host dendritic cells play a key role in organ transplant rejection. *Nat Commun.* (2016) 7:12623. doi: 10.1038/ncomms12623
67. Ochando J, Ordikhani F, Boros P, Jordan S. The innate immune response to allotransplants: mechanisms and therapeutic potentials. *Cell Mol Immunol.* (2019) 16:350–6. doi: 10.1038/s41423-019-0216-2
68. Gollmann-Tepeköylü C, Graber M, Pözl L, Nägele F, Molling R, Esser H, et al. Toll-like receptor 3 mediates ischaemia/reperfusion injury after cardiac transplantation. *Eur J Cardio-Thorac Surg.* (2020) 57:826–35. doi: 10.1093/ejcts/ezz383
69. Zhao J, Huang X, Mcleod P, Jiang J, Liu W, Haig A, et al. Toll-like receptor 3 is an endogenous sensor of cell death and a potential target for induction of long-term cardiac transplant survival. *Am J Transplant.* (2021) 21:3268–79. doi: 10.1111/ajt.16584
70. Redondo N, Rodríguez-Goncer I, Parra P, Ruiz-Merlto T, López-Medrano F, González E, et al. Influence of single-nucleotide polymorphisms in TLR3 (rs3775291) and TLR9 (rs352139) on the risk of CMV infection in kidney transplant recipients. *Front Immunol.* (2022) 13:929995. doi: 10.3389/fimmu.2022.929995
71. Redondo N, Navarro D, Aguado JM, Fernández-Ruiz M. Human genetic polymorphisms and risk of viral infection after organ transplantation. *Transplant Rev.* (2022) 36:100669. doi: 10.1016/j.trre.2021.100669
72. Cohen GS, Kallaral MA, Jayaraman S, Ibukun FI, Tong KP, Orzolek LD, et al. Transplantation elicits a clonally diverse CD8+ T cell response that is comprised of potent CD43+ effectors. *Cell Rep.* (2023) 42:112993. doi: 10.1016/j.celrep.2023.112993
73. Pinho SS, Alves I, Gaifem J, Rabinovich GA. Immune regulatory networks coordinated by glycans and glycan-binding proteins in autoimmunity and infection. *Cell Mol Immunol.* (2023) 20:1101–13. doi: 10.1038/s41423-023-01074-1
74. Siegel CH, Sammaritano LR. Systemic lupus erythematosus. *JAMA.* (2024) 331:1480–91. doi: 10.1001/jama.2024.2315
75. Flores R, Zhang P, Wu W, Wang X, Ye P, Zheng P, et al. Siglec genes confer resistance to systemic lupus erythematosus in humans and mice. *Cell Mol Immunol.* (2019) 16:154–64. doi: 10.1038/cmi.2017.160